Moreover, $\mathbf{E}_{\tau y}[a^2c^2]$ is made of terms of the kind

$$\mathbf{E}_{\tau y}\left[\begin{bmatrix} s_1 \\ p_1, q_1 \end{bmatrix}\begin{bmatrix} s_2 \\ p_2, q_2 \end{bmatrix}\begin{bmatrix} s_3 \\ p_3, q_3 \end{bmatrix}\begin{bmatrix} s_4 \\ p_4, q_4 \end{bmatrix}\right]$$

$$= \mathbf{E}_{\tau}\left[\sum_{i_1,\dots,i_4=0}^{s_1,\dots,s_4} \mathbf{E}_y[y_{i_1+p_1}^0 y_{i_2+p_2}^0 y_{i_3+p_3}^0 y_{i_4+p_4}^0]\right.$$

$$\left. \times \mathbf{E}_y[y_{i_1+q_1}^1 y_{i_2+q_2}^1 y_{i_3+q_3}^1 y_{i_4+q_4}^1]\right]$$

Whenever the map producing the spreading sequence is piecewise affine [4] a systematic tensor-based computation yields analytical expressions for the preceding terms. In particular, we may consider the family of the so-called (n, t)-tailed shifts that are known to produce spreading sequences that are optimal in reducing multiple access interference when bit error probability is the merit figure.

When these map are quantised to give zero-mean symbols we have $\mathbf{E}_y[y_0^u y_j^u] = r^j$ and $\mathbf{E}_y[y_0^u y_j^u y_k^u y_l^u] = r^{j-k+l}$ if $j \le k \le l$ and $r = -t/(n-t)$ is linked to the geometrical feature of the map.

Average performance: Exploiting these expressions for all the necessary correlations we arrive at a computable form for $\mathbf{E}_{\tau y}[D(2)]$ as a function of N and r. This allows us to investigate the performance of different choices in the family of the (n, t)-tailed shifts.

Note that the statistical behaviour of an $(n, 0)$-tailed shift $(r = 0)$ is indistinguishable from that of a generator of i.i.d. sequences. Since i.i.d is the case that most of the common methods for sequence generation aim at approximating, we will use it as a reference.

In Fig. 1 we set $N = 7$ and report the behaviour as a function of r of the three non-trivial coefficient $\mathbf{E}_{\tau y}[\alpha_2]$, $\mathbf{E}_{\tau y}[\alpha_3]$, and $\mathbf{E}_{\tau y}[\alpha_4]$ that control the dependence of $\mathbf{E}_{\tau y}[D(2)]$ on ρ. To highlight the gain with respect to the i.i.d. case, the plots are normalised with respect to their value for $r = 0$.
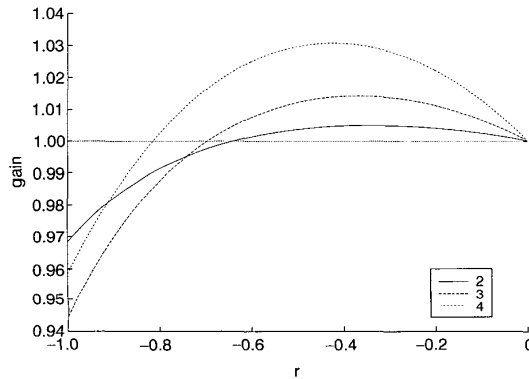

Fig. 1 *Gain in $E_{\tau y}[\alpha_2]$, $E_{\tau y}[\alpha_3]$, and $E_{\tau y}[\alpha_4]$ over i.i.d. spreading sequences against correlation decay for $N = 7$*
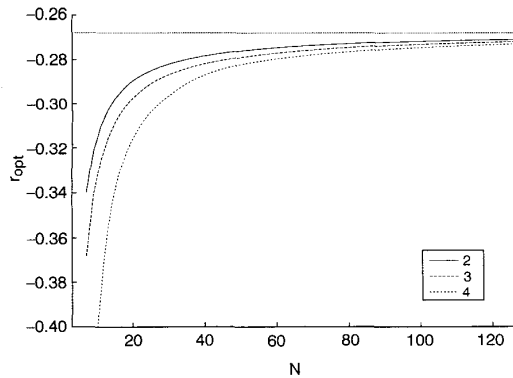

Fig. 2 *Trend of optimum correlation decay against N*

Note that all the coefficients feature an absolute maximum gain greater than 1 for a strictly negative r. Hence, maximum performance is

always achieved for negatively correlated spreading sequences though the exact value of r for which maximum performance is achieved may vary with ρ.

It is now interesting to investigate how the optimal sequence choice behaves for large N. To this aim we plot in Fig. 2 the values of r maximizing $\mathbf{E}_{\tau y}[\alpha_2]$, $\mathbf{E}_{\tau y}[\alpha_3]$, and $\mathbf{E}_{\tau y}[\alpha_4]$ for increasing values of N. Note how absolute maxima tend to accumulate in a neighbourhood of $r = -2 + \sqrt{3} = -0.268$ which is known to optimise performance also when bit error rate is the merit figure [1].

This indicates that, for large N, the best choice for spreading sequences is actually independent of ρ and entails a decay regulated by $-2 + \sqrt{3}$ which therefore seems to play a special role for asynchronous DS-CDMA systems.

References

1 MAZZINI, G., ROVATTI, R., and SETTI, G.: 'Interference minimization by auto-correlation shaping in asynchronous DS-CDMA systems: Chaos-based spreading is nearly optimal', *Electron. Lett.*, 1999, **35**, pp. 1054–1055

2 ROVATTI, R., MAZZINI, G., and SETTI, G.: 'Enhanced rake receivers for chaos-based DS-CDMA', *IEEE Trans. Circuits Syst. I*, 2001, **48**, pp. 818–829

3 ROVATTI, R., MAZZINI, G., and SETTI, G.: 'Shannon capacities of chaos-based and conventional asynchronous DS-CDMA systems over AWGN channels', *Electron. Lett.*, 2002, **38**, pp. 478–480

4 ROVATTI, R., MAZZINI, G., and SETTI, G.: 'A tensor approach to higher-order correlation of quantized chaotic trajectories – part I: General theory and specialization to piece-wise affine Markov systems', *IEEE Trans. Circuits Syst. I*, 2000, **47**, pp. 1571–1583

5 VERDÙ, S.: 'The capacity region of the symbol-asynchronous gaussian multiple access channel', *IEEE Trans. Inf. Theory*, 1989, **35**, pp. 733–751

6 COVER, T.M., and THOMAS, J.A.: 'Elements of Information Theory' (Wiley, New York, 1991), Chap. 10

Closed-loop MIMO architecture based on water-filling

Lin Dai, Shi-dong Zhou, Hai-ruo Zhuang and Yan Yao

A novel closed-loop MIMO architecture is proposed, in which channel state information is fully utilised to maximise channel capacity. Simulation results show that compared with V-BLAST, it can achieve much better performance while maintaining the same high spectral efficiency. Nearly 5 dB gain can be provided by this new architecture over V-BLAST.

Introduction: Recent information-theoretic studies have shown that substantial capacity gain can be provided by multiple-input multiple-output (MIMO) systems in a quasi-static flat Rayleigh-fading environment owing to extra degrees of freedom available within a MIMO channel [1]. An approach for exploiting this capacity potential has been proposed, known as Bell LAb vertical layered Space-Time architecture (V-BLAST) [2]. In V-BLAST systems, parallel data streams are simultaneously transmitted through multiple antennas in the same frequency band, and separated at the receiver according to their distinct spatial signatures with interference rejection and cancellation techniques. It has gained much attention owing to its high spectral efficiency and reasonable complexity. However, V-BLAST operates in an open loop, i.e. without channel knowledge at the transmitter. Better performance can be expected provided that channel

state information (CSI) is utilised to shape the transmission wave-forms. Motivated by this idea, in this Letter we develop a novel closed-loop MIMO architecture (c-MIMO) that is proved to be optimal in terms of channel capacity. It is shown that compared with V-BLAST, c-MIMO can maintain the same high spectral efficiency, but achieve much better performance owing to more effective transmission power allocation and diversity gain.

Channel model: We assume that the channel is quasi-static and flat. Each element of the channel gain matrix $\mathbf{H}$ is modelled as an independent complex Gaussian random variable with zero mean and unit variance per dimension. The noise is assumed to be complex Gaussian distributed with zero mean and variance σ_z^2 per dimension. The following notations will be used throughout this Letter: * transpose conjugate, $'$ tranpose, $\mathbf{I}_n$ the $n \times n$ identity matrix, bold lower case letters for vector, and bold upper case letters for matrix.

System description: The block diagram of our MIMO architecture is shown in Fig. 1. At the transmitter, the information is split into m parallel data streams and encoded separately. After being modulated, those streams are multiplied by a linear transformation matrix $\mathbf{K} \in \mathbf{C}^{m \times m}$ and then transmitted through m antennas. The total transmission power is assumed to be P_t, regardless of m. At the receiver, maximum likelihood decision (MLD) is adopted to achieve optimum performance. It can be seen that our c-MIMO architecture has the similar transmit structure as V-BLAST. However, we add a linear transformation $\mathbf{K}$ before transmission. The design of $\mathbf{K}$ is based on the water-filling principle that has been proved to maximise channel capacity when the channel is known at both the transmitter and the receiver [3].
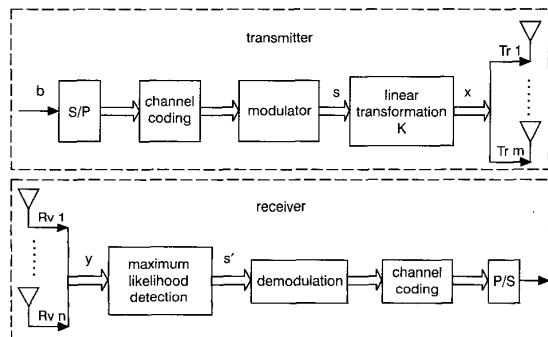

Fig. 1 *Block diagram of our novel architecture*

Design for K: Let $\mathbf{s} = [s_0, s_1, \ldots, s_{m-1}]$, represent the modulated symbol vector, where s_i's are independent symbols with equal power P_t/m. The transmitted symbol vector is then $\mathbf{x} = \mathbf{K} \cdot \mathbf{s}$, and its covariance matrix is

$$\mathbf{Q}_1 = \mathbf{KQK}^*, \quad \text{where} \quad \mathbf{Q} = E[\mathbf{ss}^*] = \mathrm{diag}(P_t/m) \qquad (1)$$

$\mathbf{Q}_1$ should also satisfy the average power constraint. Therefore $\mathbf{K}$ is requested not to change the trace of $\mathbf{Q}_1$.

By the singular value decomposition theorem, $\mathbf{H} \in \mathbf{C}^{n \times m}$ can be written as $\mathbf{H} = \mathbf{U \Lambda V}^*$ where the columns of $\mathbf{U}$ and $\mathbf{V}$ are eigenvectors of $\mathbf{HH}^*$ and $\mathbf{H}^*\mathbf{H}$, respectively. The diagonal entries of $\mathbf{\Lambda}$ are square roots of the eigenvalues of $\mathbf{HH}^*$. Thus we have

$$C = \log \det(\mathbf{I_n} + \frac{1}{\sigma_z^2} \mathbf{HQ}_1\mathbf{H}^*) = \log \det(\mathbf{I_n} + \mathbf{\Lambda} \tilde{\mathbf{Q}} \mathbf{\Lambda}')$$

where

$$\tilde{\mathbf{Q}} = \frac{1}{\sigma_z^2} \mathbf{V}^* \mathbf{KQK}^* \mathbf{V} \qquad (2)$$

From [3] we know that, when

$$\tilde{\mathbf{Q}} = \mathrm{diag}(\mu - \lambda_i^{-1})^+ \quad \text{and} \quad \sum_{i=1}^{m} \tilde{q}_{ii} = P_t/\sigma_z^2 = \rho \qquad (3)$$

$$\max C = \sum_{i=0}^{r-1}(\log(\mu\lambda_i))^+ \qquad (4)$$

where $\mathbf{a}^+$ denotes $\max\{0, \mathbf{a}\}$. r is the rank of $\mathbf{H}$. λ_i's are eigenvalues of $\mathbf{HH}^*$.

Substituting (1) and (3) into (2) yields

$$\mathbf{KK}^* = \mathbf{VDV}^* \qquad (5)$$

where

$$\mathbf{D} = \mathrm{diag}(m(\mu - \lambda_i^{-1})/\rho)^+ \qquad (6)$$

It is pointed out that the solution $\mathbf{K}$ of (5) is not unique. Let $\mathbf{W}$ be an arbitrary unitary matrix, then $\mathbf{K}$ can be written as

$$\mathbf{K} = \mathbf{VD}^{1/2}\mathbf{W} \qquad (7)$$

It can be proved that (7) satisfies the constraint condition $tr(\mathbf{Q}_1) = tr(\mathbf{Q})$. Therefore, according to (7) we can design the linear transformation $\mathbf{K}$ to maximise channel capacity.

It is pointed out that although the channel capacity is maximised as long as $\mathbf{W}$ is a unitary matrix, $\mathbf{W}$ should be carefully selected for particular coding and modulation since the error performance depends on $\mathbf{W}$. In this Letter, we search the optimal $\mathbf{W}$ to minimise the pairwise error probability, namely, to maximise the minimum distance between received vectors.

Performance results: In this Section, we evaluate the performance of c-MIMO and compare it with V-BLAST. To make a fair comparison, in our simulations we assume that MLD is also adopted in V-BLAST instead of interference rejection and cancellation. For simplicity, we limit the results in this Section to the case of uncoded QPSK modulation with $m = 2$ and $n = 2$, although c-MIMO applies to R-ary PSK with m transmitting antennas and n receiving antennas in general. Obviously c-MIMO achieves the same spectral efficiency as V-BLAST, namely, 4 bit/s/Hz. As aforementioned, $\mathbf{H}$ is considered as constant over a frame, and varies from one frame to another. Each frame consists of 130 transmissions out of each transmit antenna [4].

Fig. 2 shows the frame error rate (FER) performance of c-MIMO and V-BLAST. For comparison, we also provide their corresponding results of capacity limit, i.e. the curves of outage probability against SNR for a capacity of 4 bit/s/Hz. It can be observed that c-MIMO performs within 5 dB of the closed-loop capacity limit, which is rather striking since this is obtained without coding. Even better performance can be expected if a powerful code is adopted in c-MIMO, such as turbo code. In contrast, V-BLAST has much worse performance. c-MIMO outperforms V-BLAST by 3.2 dB at the FER of 0.10. For the FER of 0.01, the performance gain increases to 5.2 dB.
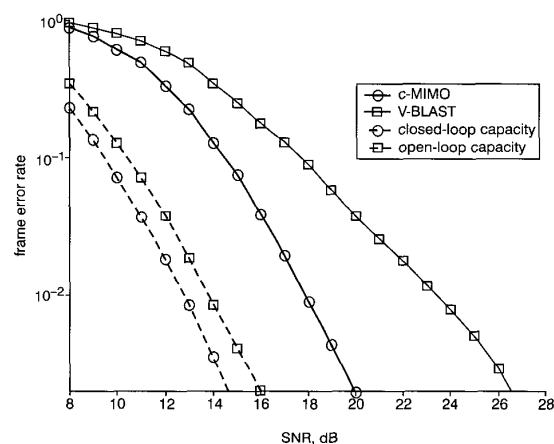

Fig. 2 *Comparison of FER performance of c-MIMO and V-BLAST (with MLD)*

Conclusion: We have presented a spectral efficient closed-loop MIMO architecture, c-MIMO, in which channel capacity is maximised. It is shown that c-MIMO cannot only achieve high spectral efficiency, but also provide remarkable error performance.

Lin Dai, Shi-dong Zhou, Hai-ruo Zhuang and Yan Yao (*State Key Laboratory on Microwave and Digital Communications, Department of Electronics Engineering, Tsinghua University, Beijing 100084, People's Republic of China*)

E-mail: dlcathy@wireless.mdc.tsinghua.edu.cn

References

1 FOSCHINI, G.J., and GANS, M.J.: 'On limits of wireless communication in a fading environment when using multiple antennas', *Wirel. Pers. Commun.*, 1998, **6**, (3), pp. 311–335

2 WOLNIANSKY, P.W., FOSCHINI, G.J., GOLDEN, G.U., and VALENZUELA, R.A.: 'V-BLAST: an architecture for realizing very high data rates over the rich-scattering wireless channel', Proc. ISSSE'98, Pisa, Italy, 1998, pp. 295–300

3 TELATAR, E.: 'Capacity of multi-antenna Gaussian channels', AT&T Bell Labs Internal Technical Memo, June 1995

4 TAROKH, V., SESHADRI, N., and CALDERBANK, A.R.: 'Space-time codes for high data rate wireless communication: performance criterion and code construction', *IEEE Trans. Inf. Theory*, 1998, **44**, (2), pp. 744–765

COFDM performance evaluation in outdoor MIMO channels using space/polarisation-time processing techniques

A. Doufexi, M. Hunukumbure, A. Nix, M. Beach and S. Armour

Outdoor physical layer performance results are presented for a proposed 4G coded orthogonal frequency division multiplexing (COFDM) system. The transceiver employs space-time processing and results are obtained using measured wideband MIMO channels. Gains as high as 10.5 dB are observed using 2Tx and 2Rx antennas for 1/2 rate coded QPSK at a PER of 10^{-2}. Additionally, results are compared for spatial and polarisation diversity.

Introduction: The combination of coded orthogonal frequency division multiplexing (COFDM) and multiple input multiple output (MIMO) signal processing is an attractive candidate for 4G wireless systems, as both space-time diversity and coding gain can be readily obtained. In this Letter we investigate the application of Alamouti's block coding scheme [1] to a COFDM system with the aid of measured MIMO channel data.

In [2], COFDM employing space-time block codes (STBC) was proposed as a potential 4G cellular standard and key-link parameters were specified. Table 1 of this Letter summarises these parameters. The individual carriers were modulated using BPSK, QPSK, or 16QAM with coherent detection. The channel encoder consisted of a 1/2 rate mother convolutional code and subsequent puncturing. The different transmission modes (comprising various coding and modulation schemes) were selected by a link adaptation scheme. It was assumed that two antennas were used in both the transmitter and the receiver. In this Letter, measured MIMO channel data is utilised to evaluate the performance of the proposed 4G space-time coded COFDM system.

**Table 1:** COFDM parameters for 4G

Parameter	Values
Operating frequency	2 GHz
Bandwidth (*B*)	4096 kHz
Useful symbol duration (*T*)	62.5 μs
Guard interval duration (T_g)	15.625 μs (T/4)
Total symbol duration (T_{symbol})	78.125 μs (with $T_g = T/4$)
Channel coding	Punctured 1/2 rate convolution code, $\{133, 171\}_{octal}$
FFT size	256
Sub-carrier spacing (Δ_f)	16 kHz

MIMO channel characterisation: An outdoor field trial campaign in the 2 GHz band was conducted in Bristol (UK) using a wideband channel sounder [3]. A 4 × 8 MIMO configuration was used in the trials, with dual polarised antenna elements employed at both transmit and receive ends. The transmit station was roof-top mounted, whilst a vehicular installation was employed for the receiver supporting both short drive and stationary measurements [3].

A high degree of decorrelation among the constituent MIMO channels is a prerequisite for achieving maximum diversity gains with block coding. Furthermore, for COFDM systems it is critical to have a long rms delay spread in the channel profile in order to obtain sufficient frequency diversity. The non-line of sight (NLOS) slow moving measurements from this urban environment fulfil both of these requirements. The correlation coefficients for these channels for an NLOS deployment are given in Table 2 for three different combinations of transmit and receive antennas. In scenario 1, the transmit antenna ports are of opposite polarisation and also spaced 20λ apart, while the receiving ports have a spatial separation of 1.5λ. Scenario 2 has only polarisation diversity at both ends. In scenario 3, only spatial diversity is employed with element separations of 20λ and 0.5λ at the transmit and receive ends, respectively.

Table 2: Comparison of channel correlation for different MIMO configurations

Scenario	Measurement MIMO outdoor	rms (ns)	Correlation Tx1, Tx2 on Rx1	Correlation Rx1, Rx2 from Tx1
1 Space and polarisation diversity	Tx1 = antenna 1 (+45°)	170	0.3763	0.3818
	Tx2 = antenna 2 (−45°)			
	Rx1 = Rx antenna 1 (+45°)			
	Rx2 = Rx antenna 4 (+45°)			
2 Polarisation diversity	Tx1 = antenna 1 (+45°)	170	0.5123	0.4866
	Tx2 = antenna 1 (−45°)			
	Rx1 = Rx antenna 1 (+45°)			
	Rx2 = Rx antenna 1 (−45°)			
3 Space diversity	Tx1 = antenna 1 (+45°)	170	0.4050	0.4106
	Tx2 = antenna 2 (+45°)			
	Rx1 = Rx antenna 1 (+45°)			
	Rx2 = Rx antenna 2 (+45°)			
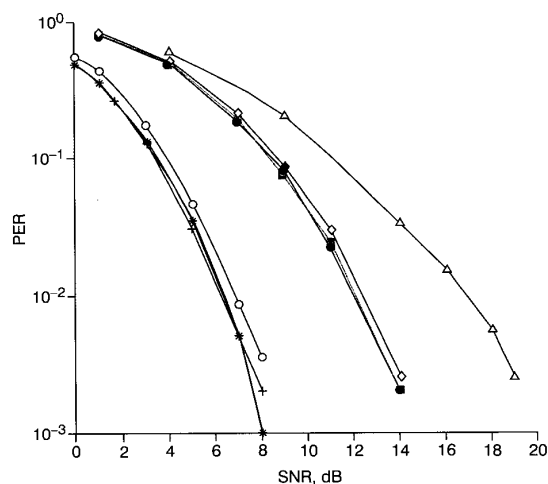
Fig. 1 *PER performance of QPSK 1/2 rate for different scenarios*

—▲— 1Tx, 1Rx
—■— 2Tx, 1Rx, scenario 1
—◆— 2Tx, 1Rx, scenario 2
—●— 2Tx, 1Rx, scenario 3
—×— 2Tx, 2Rx, scenario 1
—O— 2Tx, 2Rx, scenario 2
—+— 2Tx, 2Rx, scenario 3